Published in: Pattern Recognition Letters Volume 91, Pages 37 - 43 1 May 2017

The Version of Record is available online at: https://doi.org/10.1016/j.patrec.2017.02.002

Kurtosis and skewness at pixel level as input for SOM networks to iris recognition on mobile devices

Andrea F. Abate[a], Silvio Barra[b], Luigi Gallo[b], Fabio Narducci[b, *]

[a] University of Salerno, via Giovanni Paolo II, 132, 84084 Fisciano, Salerno, Italy
[b] ICAR - National Research Council of Italy, Via Pietro Castellino 111, 80131 Naples, Italy

a b s t r a c t

The increasing popularity of smartphones amongst the population laid the basis for a wide range of applications aimed at security and privacy protection. Very modern mobile devices have recently demonstrated the feasibility of using a camera sensor to access the system without typing any alphanumerical password. In this work, we present a method that implements iris recognition in the visible spectrum through unsupervised learning by means of Self Organizing Maps (SOM). The proposed method uses a SOM network to cluster iris features at pixel level. The discriminative feature map is obtained by using RGB data of the iris combined with the statistical descriptors of kurtosis and skewness. An experimental analysis on MICHE-I and UBIRISv1 datasets demonstrates the strengths and weaknesses of the algorithm, which has been specifically designed to require low processing power in compliance with the limited capability of common mobile devices.

1. Introduction

With the ever increasing use of mobile devices amongst the population, many biometric recognition systems have been migrated to mobile environments [12]. Among them, the recognition of the owner by the iris represents an attracting functionality to be implemented in mobile devices. Results in the field of iris recognition let assert that iris is one of the strongest and most reliable biometric trait for human identification. Experimental analysis in laboratory conditions, with controlled illumination and user's cooperation, demonstrated how much feasible is to achieve the maximum recognition performance possible. However, this is not true when moving to uncontrolled environments where noise factors (e.g., light reflections, eyelids and eyelashes, pupil dilation and so on) significantly impact on the quality of iris features to be used for a reliable biometric recognition. This consideration becomes even more critical when facing with iris recognition through mobile devices. The ubiquity of this kind of devices introduces non-trivial problems of illumination and shadow occlusions. Recognizing humans' irises in both outdoor and indoor conditions is still an open issue that is hard to solve by a single solution [2]. According to our observation, indoor and outdoor environments are significantly different from each other (almost representing two opposite problems). Indoor environments create the positive conditions for poorer effects of reflections on iris surface. The lower level of noise in such a condition facilitates the segmentation steps. On the other side, poor lighting makes the segmentation much prone to occlusions by shadows. The opposite happens in outdoor conditions where the diffused environmental light dramatically reduces the problems of shadows but introduces a significant amount of reflections. The main consequence regards the reduction of the portion of iris surface usable for recognition which, in turn, increases the level of ambiguities among human irises. A possible solution to overcome all these limitations has been proposed by Microsoft with the latest generation of Lumia devices (e.g., Lumia 950). Microsoft has introduced an iris scanning system, which is based on an infrared sensor, to unlock the device by pointing the screen in frontal position to user's eyes [3]. The scanning feature, called Microsoft Hello, seems to have the right requirements for a successful implementation on mobile devices. However, it is still not mature enough and experimental data have been not formally presented to assess the level of reliability of such a system. From a technical perspective, the migration to mobile systems reduces the availability of processing power which implies to work with low resolution images and limited sensors.

Jeong et al. [5] presented one of the real first algorithms specifically developed for mobile devices. They exploited an Adaptive Gabor Filter for extracting the iris code from a previously acquired iris image.

In [2], the recognition has been based on information of the iris combined with data of the pupil, the periocular region and the rest of the image. This method was particularly reliable against reflections and optical and motion blurring. The method in [1] exploited the spatial histograms (*spatiograms*) to verify owner identity during any kind of transaction involving the exchange of sensible data.

The above cited works exploited methods that lie in the field of the image processing, i.e. the field whose goal is to provide methods to analyse the images and try to extract discriminative features for the recognition. In this work, we explore the feasibility of using an unsupervised learning technique via Self Organizing Maps (SOM) to process and cluster iris pixels in RGB images acquired by the mobile camera. The low computational demand makes them an ideal choice to meet the limited processing power of mobile devices. The paper is organized as follows: Section 2 briefly describes the key features of a SOM network and its usage in biometrics; Section 3 presents the exploited segmentation algorithm which serves as introduction for the detailed description of the processing pipeline; Section 4 discusses the dataset used for the experimentation and presents the achieved results and Section 5 draws some conclusion and future improvements of the proposed work.

2. SOM networks in biometrics

Self-organizing map (SOM) or self-organising feature map (SOFM) represents a class of artificial neural networks (ANN) that implement unsupervised learning to produce a *map*, that is a low-dimensional discretized representation of the input space of the training samples. Also known as Kohonen maps, SOM networks differ from error-correction learning networks (e.g., backpropagation with gradient descent) since they use a neighborhood function that preserves the topological properties of the input space [9].

In the recent past, SOM networks have been efficiently used for detection and localization in color images, as described in [2] and [14]. [6] showed that clustering the pixels in an image according to color and spatial features with many SOM neural networks performed better than some existing clustering-based image segmentation methods. In the field of biometric recognition, SOM networks have been demonstrated useful for the recognition of faces from a single image [17]. [10] exploited a SOM network to produce a reliable descriptor to be used as input for a Convolutional Neural Network. [16] used self organizing maps as an alternative way of representing the face subspace. On the contrary, a very limited research have been conducted on iris recognition by SOM network.

The work by Liam et al. [11] represents one of the few attempts of proving the benefits of using SOM network for recognition of human's irises in the visible spectrum. Based on this work, we proposed an intuitive and fast approach to iris recognition by exploiting the unsupervised learning from SOM networks. The proposed algorithm, meant for iris recognition on mobile devices, works with RGB images acquired by the camera in combination with two statistical descriptor at pixel level that are *kurtosis* and *skewness*. In Section 3 a comprehensive description of the algorithm and its processing pipeline is provided.

3. Description

3.1. Segmentation

The segmentation issue has been faced by applying the method by [4] (the approach that won the iris segmentation contest MICHE-I[1]). The approach detects the iris and the pupil by means of the circular Hough transform; then, a normalization step turns the segmentation from the Cartesian coordinates to the polar coordinates. Finally, glares and eyelids are detected and discarded from the segmentation (see Fig. 1).

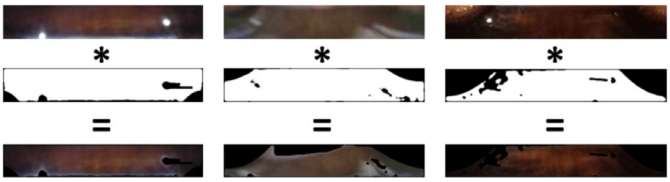

Fig. 1. Some examples of the segmentations that Haindl method produces over the images of MICHE dataset.

The main drawback of the above cited method lies on the high computing time of the segmentation mask, mainly due to the detection of defects. In fact, Haindl segmentation method computes the segmentation mask on a 400 × 300 RGB image in about 17 s on a desktop system (see Section 4 for detail on our test-bed). The higher the resolution of the image, the higher the computational demand. Since in mobile environments any feedback to the user has to be provided in the lowest time possible, such a solution to iris segmentation is hard to implement and objectively unsuitable. Therefore, we reduced the power demand by applying the preliminary steps of the algorithm only, i.e. the one implying the Hough transform to find circles in the image. This significantly reduce the time of image processing to a average time of 4.9 s on full resolution images in UBIRIS dataset (that is 800 × 600).

3.2. Recognition

Starting from the segmented iris, the image is then used to configure and train the SOM network. Such a network clusters all pixels of the image thus building the feature map of the iris. The overall architecture of the algorithm is depicted in Fig. 2.

The SOM network is fed with RGB triples of each pixel in the image but the input is not limited to that. In addition to color data, some statistical descriptors have been exploited, namely *kurtosis* and *skewness* [8], locally computed at pixel level in the image. In fact, before training the network, the algorithm computes the values of skewness and kurtosis for each pixel in a 3 × 3 neighborhood window. More precisely, the skewness is a statistical measure of the symmetry of a distribution. It can be positive, zero or negative:

1. Skewness > 0 → right skewed distribution - most values are concentrated on left of the mean, with extreme values to the right.
2. Skewness < 0 → left skewed distribution - most values are concentrated on the right of the mean, with extreme values to the left.
3. Skewness = 0 → mean = median, the distribution is symmetrical around the mean.

In a similar way to the concept of skewness, kurtosis is a descriptor of the shape of a probability distribution. More specifically, it represents the degree of *peakedness* of a distribution or, in alternative way, it is a measure of the *tailedness* of the probability distribution (see Fig. 3).

The computation of the kurtosis and skewness values at pixel level produces two alternative images of the iris which are used to feed the network, together with the RGB image. The output of the network consists in the activation status of the neural net (the feature map) which is used as a way of clustering the pixels. By using a SOM net of size 5 × 5 and two images of 600 × 100 pixels to be compared, the network is fed with each image separately to produce a new image of 600 × 100 pixels which characterizes the images clusters. On each image, the algorithm computes the Histogram of Gradients [7] which is finally used as a feature vector

[1] http://biplab.unisa.it/MICHE/index _ miche.htm

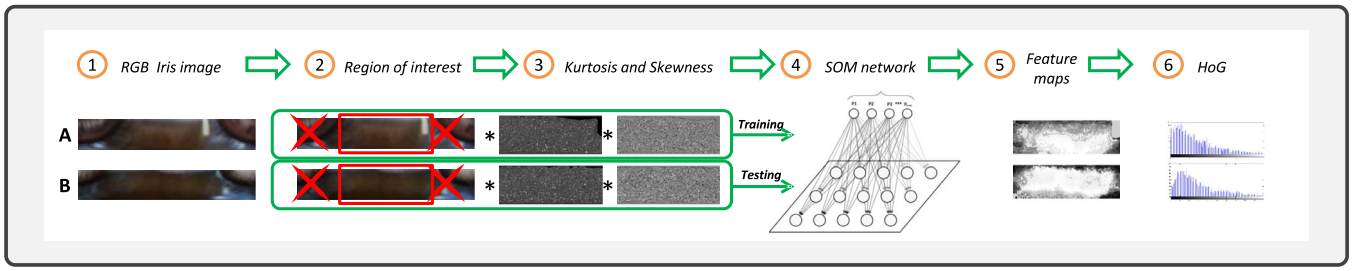

Fig. 2. The overall view of the pipeline processing of the algorithm. The architecture model shows the main steps used by the algorithm to arrive to a probability of similarity of two RGB images of users' irises.

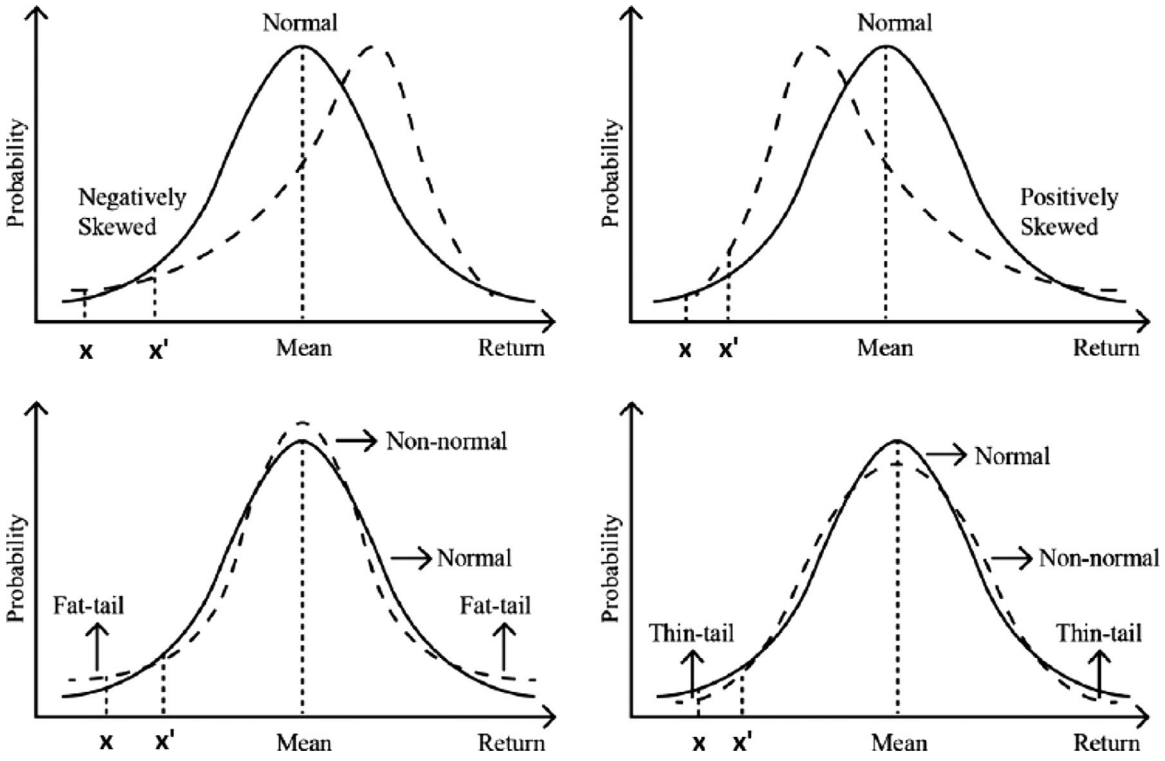

Fig. 3. The interpretation of skewness and kurtosis. The first row of the graph on the left shows a negative skewed curve and how the values of x and x changes with respect to the normal distribution. On the right the positively skewed distribution. At the bottom, the effect of low (left) and high (right) kurtosis over the normal distribution. Picture is from [18] .

representing the subject's iris. In order to measure the level of correlation between two images A and B, thus verifying the identity of the subject, the Pearson's coefficient has been calculated and it is defined as follows:

$$L = \frac{\sum_m \sum_n (A_{mn} - \bar{A})(B_{mn} - \bar{B})}{\left(\sum_m \sum_n (A_{mn} - \bar{A})^2\right)\left(\sum_m \sum_n (B_{mn} - \bar{B})^2\right)} \quad (1)$$

where $\bar{A}$ and $\bar{B}$ represent the mean values over the pixel values of the entire images. The Pearson's correlation is used as the probability measure that the two irises are from the same subject or not. Comparisons that produce a correlation coefficient close to 1 indicate that the images are irises of the same subject and viceversa when the output is close to 0.

4. Experiments

4.1. Iris datasets

The proposed method was evaluated on two different datasets: the first is an extended version of the publicly available MICHE-I dataset (hereafter MICHE) [13]), released for the evaluation phase of the MICHE-II competition held at ICPR 2016. The images in the dataset have been acquired from 90 subjects with using two different mobile devices: an iPhone (hereinafter IP5) and a Galaxy Samsung IV (hereinafter GS4). For each subject, at least four images have been collected. The images in the dataset are affected by several noise factors: illumination changes, semi-closed eyes and reflections. Their presence increases the difficulty in locating the iris area so dramatically degrading the quality of the extracted biometric trait. Also, since the images are acquired with three different devices, the recognition phase becomes even more challenging, due to the complications brought by the cross-device comparisons. In Fig. 4 some of the issues discussed above are shown; in the first row the subjects kept their eyes wide opened, simplifying a correct detection and the following segmentation of the iris, both in indoor (1st, 4th, 5th, and 6th image in the row) and in outdoor conditions (2nd and 3rd image in the row). On the contrary, in the second row, several conditions make very difficult the detection of the area-of-interest: out-of-axis irises (1st and 4th image), reflections (1st and 6th image), semi-closed eyes (2nd and 3rd image) and adverse lighting conditions (5th image). Such factors seriously compromise the recognition phases.

Fig. 4. Several examples of the images composing the MICHE dataset. The images in the first row offer advantageous conditions for the detection of the iris; on the contrary, those in second row are affected by several kinds of noise.

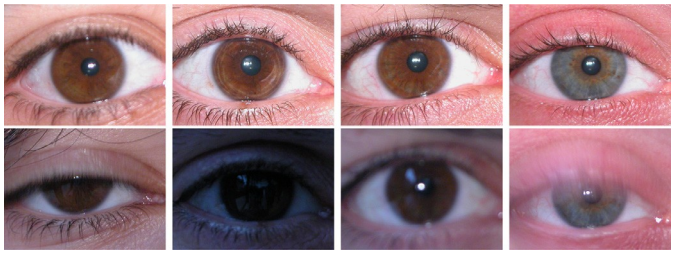

Fig. 5. The figure above shows some examples of the UBIRIS dataset. Whereas the images in the first session (first row) are acquired in controlled condition of lighting, those in the second session (second row) are more challenging segment due to casual blurring and natural illumination.

The second dataset is UBIRISv1 (hereafter UBIRIS) from the SOCIALab of UBI (University of Beira Interior) [15]. The dataset contains five images acquired from 241 subjects in indoor environment. The choice of this specific set of images is due to the acquisition policy adopted. In fact, whereas in the first session (first row in Fig. 5), most noise factors are minimized, especially those related to the illumination and the reflections, in the second one (second row in Fig. 5) the capture location has changed in order to introduce a natural luminosity factor. The full resolution of images in UBIRIS are significantly lower than the standard features of cameras equipped on mobile devices. This condition makes the dataset as a suitable reference for assessing the performance of the proposed algorithm in presence of more cooperative users (since all images are almost planar to the camera).

4.2. Interpretation of SOM output

The experiments have been simulated by MATLAB 2013a on commodity hardware, a Microsoft Windows machine equipped with an Intel(R) Core(TM) Duo CPU P8600 @ 2.40GHz. The selected machine features a processing power that is comparable with the average CPU performances of current mobile devices, thus providing a reasonable estimate of the time consumption of the algorithm when running on mobile systems. Fig. 6 shows neurons information when the network is configured and trained on each image. The distances between pairs of neurons can be seen as the low dimensional representation of subject's iris. In more details, in the picture is shown a net of dimension 5×5 (25 neurons) which divides the iris pixels into 25 different clusters. Observing the distance patterns between neighboring neurons, it can be noticed how they differ among subjects. We used this information as a key reference to distinguish users between each other. Fig. 7 clarify how the activation status of each one of 25 neurons of the network exhibits a similar trend for two acquisitions of the same

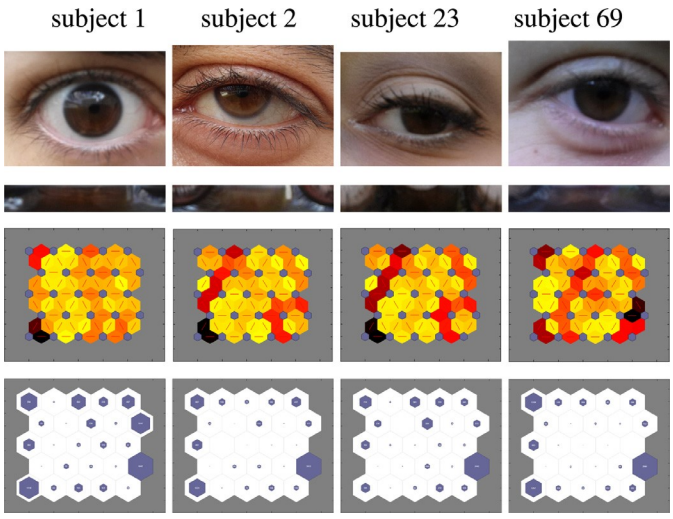

Fig. 6. Examples of SOM network configurations on acquisition of different subjects. In the third line the computed distances between the neighboring neurons are shown. The fourth shows the cluster decomposition of the image. These information can be interpreted as the low dimensional representation of subjects' irises.

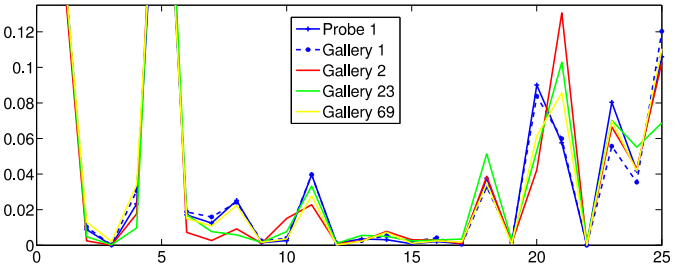

Fig. 7. Mean activation (y axis) status of 5×5 (i.e. 25, x axis) SOM neurons when the training phase is performed over Subject 1 and the output of the network are from subject 1, 2, 23 and 69, respectively.

subject (Probe1 and Gallery1 in the figure) with respect to that obtained with different subjects, that are Gallery2, Gallery23 and Gallery69 respectively.

4.3. Results

In this section we present the experimental results achieved on MICHE and UBIRIS datasets. The analysis is presented in terms of Recognition Rate (hereafter RR), Equal Error Rate (EER), Area Under Curve (AUC) and Decidibility (DEC). Preliminary results obtained on an extended version of MICHE dataset (made available during the MICHE-II ICPR 2016 contest) have been collected to assess the reliability of the proposed method. Two different network models have been considered, that are 5×5 and 10×10 which mean 25 and 100 neurons respectively. A collection of pictures from MICHE dataset, representing the test dataset used for the contest, has been used. More precisely, probe and gallery sets were populated with 30 different subjects. The first experiment has been performed on images acquired in indoor conditions by iPhone 5 (hereafter IP5). The second one has been carried out on images by Samsung Galaxy S4 (hereafter GS4) in outdoor conditions. In both experiments the frontal camera has been considered. Although the sensor mounted on the rear camera of mobile devices offers better resolution and image quality in general, it is rather uncommon and impractical to use for iris recognition. Experimental results have been summarised in Table 1. We can observe that in mean, the performance of the algorithm are better for IP5 than for GS4. In particular, the algorithm achieves 87% of recognition rate using a 5

Table 1
Performance results of the proposed method, when images from IP5 and GS4 are compared.

Network model	IP5 versus IP5			GS4 versus GS4		
	RR	AUC	EER	RR	AUC	EER
5 × 5	0 .87	0 .93	0 .13	0 .63	0.88	0 .21
10 × 10	0 .83	0 .92	0 .12	0 .76	0.88	0 .21

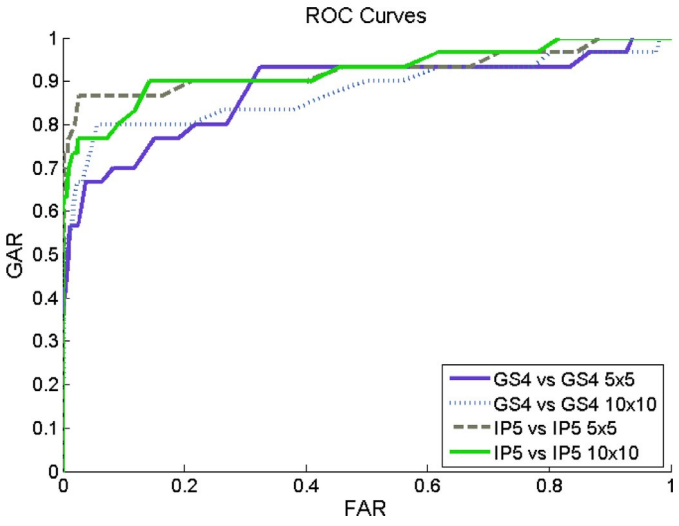

Fig. 8. (top) ROC curves of the experiments with two SOM models; (bottom) the probability distributions of genuine and impostors in all experiments.

Table 2
The table shows the results obtained on UBIRIS dataset by applying three different scale factors and fixing the net size to be 10 × 10.

Net size	Dataset	S/F	RR	EER	AUC	DEC
10 × 10	UBIRIS	0 .25	0 .90	0.06	0.98	2 .92
10 × 10	UBIRIS	0 .50	0 .86	0.08	0.97	2 .90
10 × 10	UBIRIS	1 .00	0 .85	0.07	0.99	1 .45

× 5 net over the IP5 images, with a AUC (Area Under ROC Curve) value of 97%. On the contrary, the experiment executed over the GS4 achieves 76% of recognition rate. This is more evident in Fig. 8, which shows the ROC (Receiver Operating Characteristic) curve obtained for each experiment.

To go deeper into the first results of the ICPR 2016 contest, we extended the experiments to all subjects in the public version of the MICHE dataset as well as involving another dataset, i.e., the UBIRIS (both are better described in Section 4.1). The new session of experiments aimed at verifying relevant aspects tied to the intrinsic characteristics of the proposed SOM net. First of all, it has been necessary to assess more deeply the consequences related to the changes in resolution of iris images. In order to analyse this aspect, a 10 × 10 network has been trained over the images of UBIRIS scaled at three different resolutions:

- 0.25, i.e. a quarter of the original size of the image;
- 0.50, i.e. the half of the original size of the image;
- 1.00 (None), i.e. the image at its actual resolution.

The results obtained are summarised in Table 2; the related ROC curves are shown in Fig. 9. The gap of performance among the treatments is not significantly wide. However, a soft improvement is visible when the SOM network is trained using lower resolution images (90% of recognition rate with an EER value of 0.06%). This suggests that, as for the dataset considered, a lower resolution reduces the ambiguities by preserving the features that produce a discriminative clustering of iris pixels.

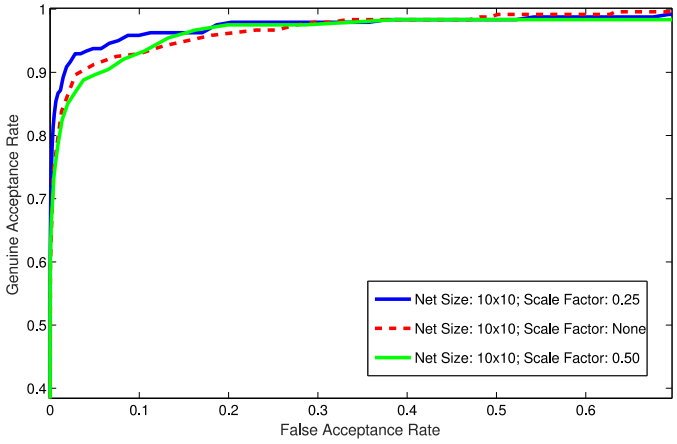

Fig. 9. ROC curves related to the experiment aimed at verify the impact of the scaling factor on the recognition performance.

Table 3
The table shows the results obtained on UBIRIS dataset by applying a scale factor of 0.25.

Net size	Dataset	S/F	RR	EER	AUC	DEC
5 × 5	UBIRIS	0.25	0 .95	0 .05	0.98	2 .84
10 × 10	UBIRIS	0.25	0 .90	0 .06	0.98	2 .92
15 × 15	UBIRIS	0.25	0 .90	0 .06	0.98	2 .90
20 × 20	UBIRIS	0.25	0 .64	0 .14	0.94	1 .30

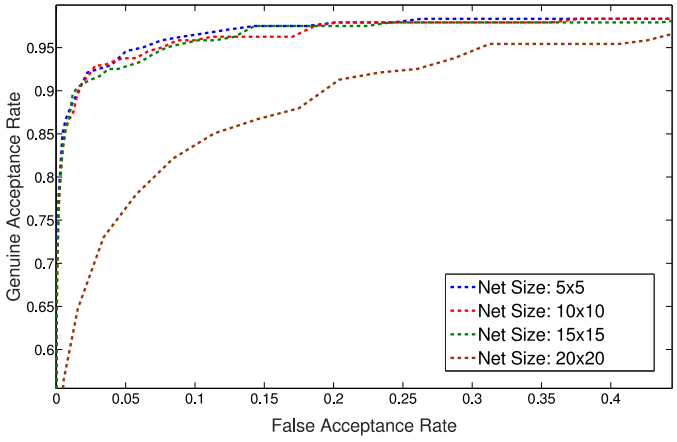

Fig. 10. ROC curves related to the experiment aimed at verify the impact that the net size has on the recognition performance.

According to this last observation, we set up a new round of experiments by fixing the scale factor at a quarter of the original resolution (that produced the best result in the previous experiment) with the aim of testing the impact of the net models over the recognition performance. We trained four different networks, namely 5 × 5, 10 × 10, 15 × 15 and 20 × 20. The results have been collected in Table 3 and shown in Fig. 10 in terms of ROC curves.

We can observe that on increasing the size of the feature map, the recognition fails. In the treatment with network model 20 × 20, the RR achieved (64%) is sensibly lower than the one obtained with smaller networks (95% and 90%). This is an encouraging result because the computation demand drops much more than linearly (Section 4.4 reports a brief analysis of the computational demand and time required). The consideration drawn so far applies rather well at the UBIRIS dataset. The good quality of segmentation provided (except for cases of noisy acquisitions which impact on the recognition performance achievable by using iris data

Table 4
The table shows the results obtained on MICHE dataset by applying three different scale factors, but fixing the net size to be 5 × 5. The portion of the dataset considered is that acquired by GS4 in outdoor condition by the frontal camera.

Net size	Dataset	S/F	RR	EER	AUC	DEC
5 × 5	MICHE	0 .50	0.67	0.26	0 .85	1 .49
5 × 5	MICHE	1 .00	0.65	0.22	0 .87	1 .49
5 × 5	MICHE	0 .25	0.63	0.25	0 .85	1 .57

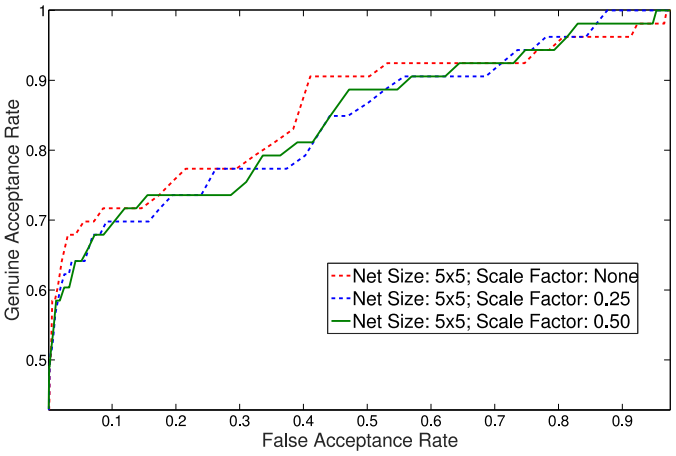

Fig. 11. ROC Curves related to the experiment aimed at verify the impact of the scaling factor on the recognition performance.

Table 5
The table shows the results obtained on MICHE dataset by applying a scale factor of 0.50.

Net size	Dataset	S/F	RR	EER	AUC	DEC
5 × 5	MICHE	0 .50	0 .67	0 .26	0.85	1 .49
15 × 15	MICHE	0 .50	0 .65	0 .18	0.89	1 .80
10 × 10	MICHE	0 .50	0 .63	0 .24	0.81	1 .17

only) and the original resolution of the acquisitions are widely responsible for such a result. We applied an analogous rationale on MICHE dataset. Compared to the previous dataset, MICHE is particularly challenging due to the presence of a wide range of noise factors. Moreover, since acquisitions have been performed in less controlled conditions, many irises present problems of out-of-focus and/or out-of-frame. In view of these considerations, the results were expected to be significantly worse than the one obtained on UBIRIS dataset. Starting from the outcomes of the previous experiments, we firstly set up a new experimental session by fixing the size of the SOM network and by changing the scale factor of image resizing. The portion of the dataset considered in this study relies on the acquisitions of all 75 subjects by GS4 in outdoor condition using the frontal camera of the device. We trained a 5 × 5 network (that have turned out to be the best size in the previous experiments) over the scaled images. In terms of RR, we obtained the best configuration with images scaled at a half of the original size. More detailed results are organized in Table 4 and the related ROC curves are depicted in Fig. 11.

Last experiment takes into account the best resulting scale factor obtained in the previous tests and aims at verifying the best performing network size on MICHE dataset. Therefore, three different SOM models have been trained: 5 × 5, 10 × 10 and 15 × 15. Numerical results are displayed in Table 5, together with the related ROC curves (see Fig. 12). Observing the performance achieved on MICHE, the SOM network of size 5 × 5 confirms to be, on average, the most reliable solution with a good trade-off among

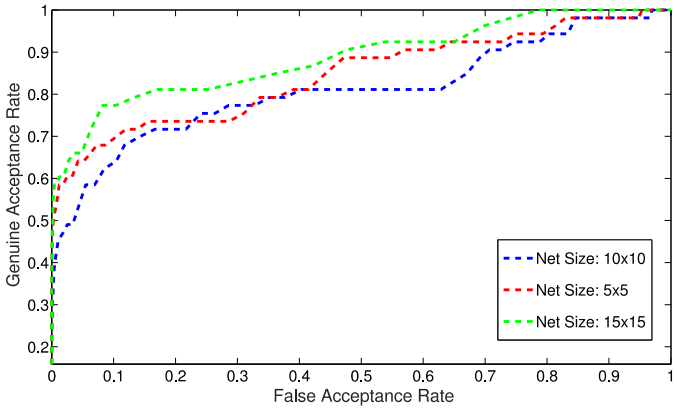

Fig. 12. ROC Curves related to the experiment aimed at verify the impact that the net size has on the recognition performance.

performance and processing demand. On the other hand, the reported results also confirms the inherent difficulties of processing MICHE iris images. The interpretation of the achieved results takes into account that all subjects in the public version of the dataset have been considered. The high impact of disturbing factors leads to a poor mean quality of the segmentation masks and iris normalizations. This lets assume that, with special regard to MICHE-like datasets, the biometric approaches that are exclusively tailored on iris data cannot achieve high performance levels. Extending the search space to periocular data might contribute to raise the accuracy and robustness of the proposed system.

4.4. Time/computing demand

Starting from the segmentation by [4], which produces an iris normalization of 600 × 100 pixel, the time spent for discarding the peripheral sectors of iris is negligible. On average, the time demand for the pre-processing of the image (which includes scaling at half size and computing kurtosis and skewness) is 2.83 s. An amount of time of 5.92 s is indeed spent for configuring and training the SOM network whose size is 5 × 5. The time spent for the comparisons of the output of the SOM network is about 0.8 s in mean, which can be considered in line with real-time processing. We deeply investigated how much significantly the performance of the proposed method are affected by the size of the image and the number of neurons. We discovered that even when scaling at 1/4 of the original size and using a simple network of 5 × 5 neurons, the performance are sensibly high. This allows to notably reduce the time and computing demand meeting the real-time requirements. The mean demand of time increases of 15% in 10 × 10 network over the one measured for 5 × 5. Moreover, it must be considered that modern mobile phones are equipped with multi-core processors and offer GPU power which enables to parallel programming. This lets suppose that the processing time could be further significantly reduced. If the preparation of the SOM network would take place at the time of the user's enrollment, the time involved in the configuration of the algorithm would be performed and stored one time only thus suppressing the time demand at that for the execution of the network and the computation of the similarity score.

5. Conclusions

In this paper, we have presented an algorithm for iris recognition that uses Self Organizing Maps (SOM) as a way of representing humans' iris in a low 2-dimensional space. SOM networks implement unsupervised learning techniques which makes them suitable for mobile devices and personal authentication systems. The

proposed approach, which works at pixel level, combines the RGB triples in the visible spectrum of each iris pixel with the statistical descriptors of kurtosis and skewness computed on a neighborhood window. The 5-tuple obtained is used as input at the SOM network to train it over the specific subject. By comparing the output of a feature-map trained on a subject against irises of other subjects, the proposed method produces a similarity score thus achieving the biometric recognition. The experimental results obtained on different SOM models (with a different amount of neurons and variable scale factors of the original image containing the iris pixels) on MICHE and UBIRIS datasets allowed to emphasize the feasibility of the proposed method as well as its weaknesses. The experimental analysis has shown that the size of the network does not necessarily imply an improvement of performance. On the contrary, in presence of good quality segmented irises, a strong reduction of original resolution does not affect the achievable level of performance. This emphasizes the central importance of a strong and reliable segmentation algorithm which is able to accurately detect and segment the iris pixels in noise images in adverse conditions. On the other side, the observations drawn on experimental data let suppose that ubiquitous iris recognition for mobile devices cannot ignore the usage of information that goes beyond the solely iris data. Expanding the analysis to periocular information can be therefore considered as a valid option for further enhancements of this study. Modern mobile architectures mount parallel hardware which can considerably decrease the time demand. Considering the high chances of parallelism of the proposed approach, we aim at optimizing the processing pipeline to further reduce the time demand thus achieving true real-time performances.

Supplementary material

Supplementary material associated with this article can be found, in the online version, at doi: http://dx.doi.org/10.1016/j.patrec.2017.02.002

References

[1] S. Barra, A. Casanova, F. Narducci, S. Ricciardi, Ubiquitous iris recognition by means of mobile devices, Pattern Recognit. Lett. 57 (2015) 66–73. http://dx.doi.org/10.1016/j.patrec.2014.10.011 . Mobile Iris {CHallenge} Evaluation part I (MICHE I).

[2] D.-H. Cho, K.R. Park, D.W. Rhee, Y. Kim, J. Yang, Pupil and iris localization for iris recognition in mobile phones, in: Seventh ACIS International Conference on Software Engineering, Artificial Intelligence, Networking, and Parallel/Distributed Computing (SNPD'06), 2006, pp. 197–201, doi: 10.1109/SNPD-SAWN.2006.58 .

[3] R. Gupta , P. Sehgal , A survey of attacks on iris biometric systems, Int. J. Biom. 8 (2) (2016) 145–178 .

[4] M. Haindl, M. Krupika, Unsupervised detection of non-iris occlusions, Pattern Recognit. Lett. 57 (2015) 60–65. http://dx.doi.org/10.1016/j.patrec.2015.02.012 . Mobile Iris {CHallenge} Evaluation part I (MICHE I).

[5] D.S. Jeong , H.-A. Park , K.R. Park , J. Kim , Iris recognition in mobile phone based on adaptive gabor filter, in: International Conference on Biometrics, Springer, 2006, pp. 457–463 .

[6] Y. Jiang, Z.-H. Zhou, Som ensemble-based image segmentation, Neural Process. Lett. 20 (3) (2004) 171–178, doi: 10.1007/s11063- 004- 2022- 8 .

[7] O.L. Junior, D. Delgado, V. Goncalves, U. Nunes, Trainable classifier-fusion schemes: an application to pedestrian detection, in: 2009 12th International IEEE Conference on Intelligent Transportation Systems, 2009, pp. 1–6, doi: 10.1109/ITSC.20 09.530970 0 .

[8] T.-H. Kim, H. White, On more robust estimation of skewness and kurtosis, Finance Res. Lett. 1 (1) (2004) 56–73. http://dx.doi.org/10.1016/S1544-6123(03)0 0 0 03-5 .

[9] K. Kiviluoto , Topology preservation in self-organizing maps, Helsinki University of Technology, 1995 .

[10] S. Lawrence , C.L. Giles , A.C. Tsoi , A.D. Back , Face recognition: a convolutional neural-network approach, IEEE Trans. Neural Netw. 8 (1) (1997) 98–113 .

[11] L.W. Liam , A. Chekima , L.C. Fan , J.A. Dargham , Iris recognition using self-organizing neural network, in: Research and Development, 20 02. SCOReD 20 02. Student Conference on, IEEE, 2002, pp. 169–172 .

[12] M.D. Marsico, C. Galdi, M. Nappi, D. Riccio, Firme: face and iris recognition for mobile engagement, Image Vis. Comput. 32 (12) (2014) 1161–1172. http://dx.doi.org/10.1016/j.imavis.2013.12.014 .

[13] M.D. Marsico, M. Nappi, D. Riccio, H. Wechsler, Mobile iris challenge evaluation (miche)-i, biometric iris dataset and protocols, Pattern Recognit. Lett. 57 (2015) 17–23. http://dx.doi.org/10.1016/j.patrec.2015.02.009 . Mobile Iris {CHallenge} Evaluation part I (MICHE I).

[14] S. Ong, N. Yeo, K. Lee, Y. Venkatesh, D. Cao, Segmentation of color images using a two-stage self-organizing network, Image Vis. Comput. 20 (4) (2002) 279–289. http://dx.doi.org/10.1016/S0262-8856(02)0 0 021-5 .

[15] H. Proença , L.A. Alexandre , Ubiris: a noisy iris image database, in: International Conference on Image Analysis and Processing, Springer, 2005, pp. 970–977 .

[16] X. Tan , S. Chen , Z.-H. Zhou , F. Zhang , Recognizing partially occluded, expression variant faces from single training image per person with som and soft k-nn ensemble, IEEE Trans. Neural Netw. 16 (4) (2005) 875–886 .

[17] X. Tan , S. Chen , Z.-H. Zhou , F. Zhang , Face recognition from a single image per person: a survey, Pattern Recognit. 39 (9) (2006) 1725–1745 .

[18] Y. Wan, M.L. Clutter, B. Mei, J.P. Siry, Assessing the role of u.s. timberland assets in a mixed portfolio under the mean-conditional value at risk framework, Forest Policy Econ. 50 (2015) 118–126. http://dx.doi.org/10.1016/j.forpol.2014.06.002 .